Kinematic models of fluvial terraces over active detachment folds: Constraints on the growth mechanism of the Kashi-Atushi fold system, Chinese Tian Shan

K.M. Scharer[†]
Department of Geological Sciences, 1272 University of Oregon, Eugene, Oregon 97403, USA

D.W. Burbank[‡]
Department of Earth Science, University of California, Santa Barbara, California 93106-9630, USA

J. Chen[§]
State Key Laboratory of Earthquake Dynamics, Institute of Geology, China Seismological Bureau, P.O. Box 9803, Beijing 100029, People's Republic of China

R.J. Weldon II[#]
Department of Geological Sciences, 1272 University of Oregon, Eugene, Oregon 97403, USA

ABSTRACT

During detachment folding, the relationship between differential uplift and shortening depends on the mechanism of fold growth, such as limb rotation or hinge migration, and may vary over the lifetime of a fold. Thus, neither long-term shortening rates nor the present fold geometry unambiguously constrain the kinematics of fold growth. Where rivers cut through growing anticlines, flights of abandoned fluvial terraces act as passive kinematic markers. As shortening progresses, the terraces become deformed and thereby preserve critical information about the kinematics and evolution of active fold growth. To constrain recent fold growth across three detachment folds in the Kashi-Atushi fold system in the SW Tian Shan, China, we surveyed flights of deformed terraces and compared them with geometric models of successively emplaced horizontal unconformities (terraces) across pregrowth strata deformed by hinge migration, limb rotation, and a combination of the two. Migration of angular hinges and curved hinge zones were also compared. Each kinematic model predicts both a distinct geometry for the deformed terraces and contrasting angular relationships between the terraces and the pregrowth strata. Notably, limb rotation and migration of curved hinge zones result in progressively rotated terraces that cut across pregrowth strata, whereas all limb-lengthening models result in parallelism between pregrowth strata and terrace straths across much of the fold. The Kashi-Atushi terraces show clear evidence of abandoned axial surfaces, concentrated deformation near the core of the folds, and progressive tilting with age. When compared to the model predictions, the folds are likely growing by a combination of limb rotation in the tight cores of the folds and hinge-zone migration of pregrowth strata across the flanks of the folds.

Keywords: strath terrace, active folding, intracontinental mountains, fault-related fold, landform evolution.

INTRODUCTION

Deformed strata deposited before folding initiates cannot unambiguously constrain the kinematics of fold growth (Jamison, 1987). Therefore, either growth strata (e.g., Suppe et al., 1992; Poblet et al., 1997) or kinematic markers formed during folding are needed to understand how folds grow and to reveal whether a consistent kinematic pattern or an evolving one accounts for the presently observed fold geometry. During the past two decades, a broad suite of models for folding was designed to explore the development of hydrocarbon reservoirs, potential seismic hazards related to faulting or folding, and the evolution of fold-and-thrust belts (e.g., McClay, 2004; Allmendinger and Shaw, 2000). Many of the models are predicated on the concept that, during folding, rocks migrate through axial surfaces that separate domains of the fold with different dips (kink bands). The models predict that over time, an axial surface can evolve from an "active" hinge, across which rocks are being folded, to a "passive" hinge, which is being inactively translated or deformed (Suppe, 1983; Suppe and Medwedeff, 1990; Poblet and McClay, 1996). In comparison to actual folds, most of these models are geometrically simple and make clear predictions about when an axial surface would be active or passive. In more complex, actual folds, the duration and timing of activity on axial surfaces is not so clear. From present-day fold geometry, it is commonly impossible to tell whether multiple axial surfaces were simultaneously active, whether axial surfaces were ever reactivated, or whether they continued to deform even when in a geometry presumed to be "passive" based on the structural models.

To remedy this problem, a suite of successively created kinematic markers is needed to define the location and magnitude of sequential deformation. This paper shows how fluvial terraces can be used as kinematic markers to differentiate between mechanisms of detachment fold growth. It is important to differentiate

[†]Present address: Department of Geology, Appalachian State University, 572 Rankin Science Building, Boone, North Carolina 28608, USA; e-mail: scharerkm@appstate.edu.
[‡]E-mail: burbank@crustal.ucsb.edu.
[§]E-mail: chenjie@eq-igl.ac.cn.
[#]E-mail: ray@uoregon.edu.

GSA Bulletin; July/August 2006; v. 118; no. 7/8; p. 1006–1021; doi: 10.1130/B25835.1; 13 figures; Data Repository item 2006142.

between mechanisms, because during detachment folding, differential rock uplift is not a simple function of shortening, but also depends on the mechanism of folding: limb rotation, hinge migration, or combinations of both (Fig. 1; Poblet and Hardy, 1995; Poblet and McClay, 1996). Moreover, the folding mechanism may change as a fold evolves. Consequently, the height of an abandoned terrace above its original base level lacks a simple, consistent, or predictable relationship to the magnitude of shortening across a fold since the terrace was created. In this paper, we show how the geometry of a flight of terraces can capture the progressive strain path and be used to deconvolve the uplift, shortening, and kinematic evolution of a growing detachment fold.

Although growth strata have successfully been used in previous studies as kinematic markers of fold growth (e.g., Medwedeff, 1989; Suppe et al., 1992; Storti and Poblet, 1997), flights of fluvial terraces provide a unique signature that requires neither seismic-reflection data nor preservation of observable growth strata. In addition, river terraces record deformation above base level and provide kinematic information in a region where growth strata may not be deposited or preserved, such as when regional erosion outpaces differential subsidence and sediment accumulation. Even where growth strata are preserved in outcrop, they are commonly missing across the core of a fold. In contrast, fluvial terraces may extend across an entire fold and can record incremental deformation. Furthermore, as dateable surfaces, terraces can be used to determine shorter-term (10–300 k.y.) shortening and uplift rates and thus quantify the patterns of strain across active detachment folds.

Combined field and modeling studies have investigated the kinematics of terraces deformed by fault-bend folds, fault-propagation folds, and folding by limb rotation (Ishiyama et al., 2004; Vannoli et al., 2004; Lavé and Avouac, 2000; Thompson et al., 2002; Molnar et al., 1994; Rockwell et al., 1988), but the kinematics of terrace deformation over detachment folds are relatively unexplored. Near the city of Kashi (Kashgar) in northwest China (Fig. 2), active shortening at 2–9 mm/yr along the southwest margin of the Tian Shan is interpreted to result from detachment folding based on the overall geometry, fault-plane solutions, mechanical stratigraphy, and absence of significant emergent faults (Scharer et al., 2004). Within water gaps across three anticlines, flights of abandoned fluvial terraces that span both limbs of the folds are nested and tilted, thereby recording evidence independent of the structural geology for the progressive evolution of the folds (Fig. 3). After presenting four models applicable to the kinematics of detachment folding, we discuss the deformation of the surveyed terraces, and close with a discussion of the kinematic history of the Kashi-Atushi folds.

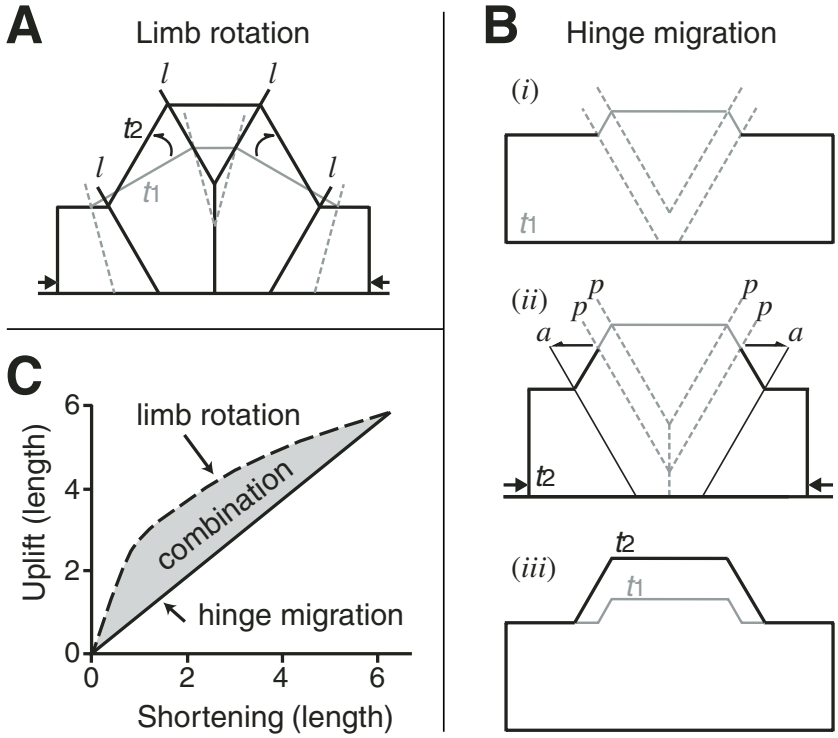

Figure 1. Kinematic models of detachment fold growth showing progressive geometry and motion of axial surfaces over time (t_1 to t_2) (after Poblet and McClay, 1996). (A) During limb rotation, the fold amplitude increases while the wavelength decreases if bed length and thickness are maintained. As the limbs tilt, and the axial surfaces rotate, a limited amount of strata passes through the axial surfaces (*l*) to maintain constant bed thickness. (B) During hinge migration, strata pass through the outer axial surfaces and into the fold, which grows in amplitude and wavelength with a constant bed thickness and limb angle. (*i*) Fold shape at t_1. (*ii*) From t_1 to t_2, the original axial surfaces (hinges) become passive (*p*) and ride up the fold with their neighboring strata as the active axial surfaces (*a*) translate outward. (*iii*) The folds grow in a self-similar manner, growing taller and wider while accommodating shortening. (C) Uplift is proportional to shortening during hinge migration but variable during limb rotation. A combination of mechanisms will follow a path in between the end-member models.

DETACHMENT FOLDING

Detachment folds form above a subhorizontal fault where shortening terminates or decreases (Dahlstrom, 1990; Mitra, 2003). Weak strata above the detachment horizon, commonly salt or gypsum deposits, accommodate shortening in the core of the fold by passive flow (ductile) deformation, while mechanically stronger, but younger overlying strata fold by flexural slip. Detachment folds are therefore associated with strong contrasts in mechanical stratigraphy and generally are not associated with significant faults exposed at the surface.

Most kinematic models for detachment fold growth appeal to two end-member mechanisms: limb rotation and hinge migration (Fig. 1). Both end members are commonly modeled as kink-band folds, with axial surfaces that sharply bisect kink bands composed of consistent dip domains. In limb rotation models, the limb length remains constant while the fold height is amplified by rotation of the limbs (Poblet and McClay, 1996; Mitra, 2003; Epard and Groshong, 1995). If constant strata thickness and limb length are required during limb rotation, axial surfaces have "limited activity," meaning that a small amount of strata migrates through the hinge as it rotates. In hinge migration models, the fold grows wider and taller by translation of the "active" hinges through the strata (Suppe et al., 1997; Poblet and McClay, 1996; Mitchell and Woodward, 1988; Mitra, 2003). The fold limbs lengthen with constant thickness as material passes through the active hinge into the limbs of the fold. These end-member mechanisms can be

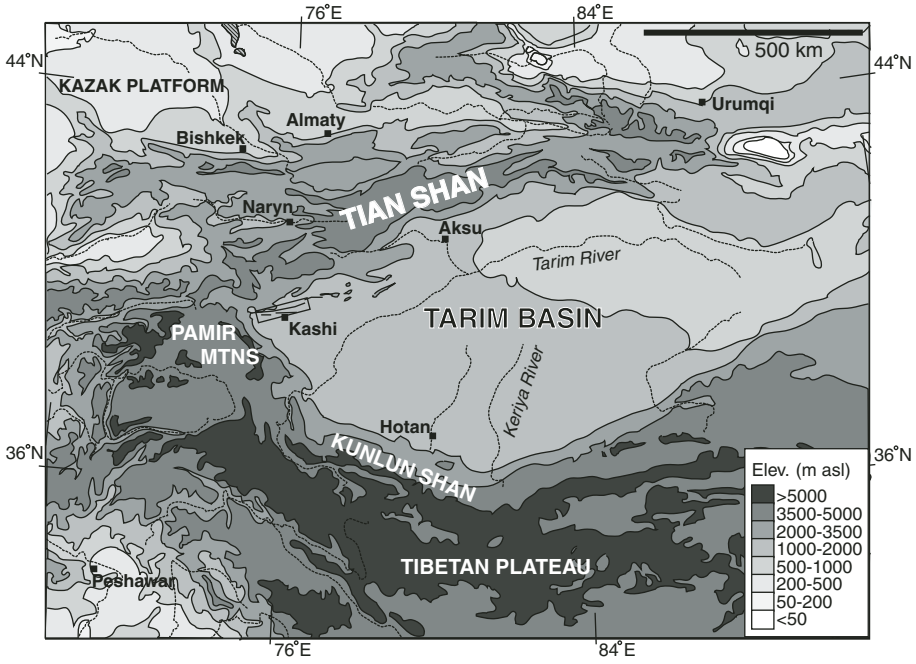

Figure 2. Topographic and geographic map of Central Asia. The Kashi-Atushi fold system (small rectangle north of Kashi) is located at the far western end of the southern Tian Shan, proximal to the Pamir indenter.

combined to produce complicated fold histories and geometries (Casas-Sainz et al., 2002; Novoa et al., 2000; Storti and Poblet, 1997).

Recognizing that the angular geometry of kink bands bisected by axial surfaces is idealized, several researchers have considered curved-hinge or curved-fault geometries undergoing hinge migration (Novoa et al., 2000; Suppe et al., 1997). Limb lengthening with wide, curved hinge zones (rather than a sharp, bisecting axial surface) results in gross geometries similar to those produced by angular hinges but that display subtle differences preserved within the curved hinge zone. When suites of fluvial terraces are superimposed on the kinematic predictions of these diverse folding models, the ensuing geometry of the deformed terraces places constraints on the permissible fold evolution.

MODEL ASSUMPTIONS

For our kinematic modeling, a terrace is represented as an originally horizontal line and is deformed passively by the process prescribed by the folding mechanism. The models are applied to braided streams with modern gradients of 0.5° to 1°, so a horizontal line is an acceptable approximation. In general, the river responsible for creating a terrace is envisioned as flowing perpendicular to the fold axis. The modeled terraces are lifted instantaneously above the graded fluvial profile due to growth of the fold. We assume that formation of terraces is a punctuated process that generates surfaces that can be treated as isochronous. For our models, an entire terrace surface is abandoned simultaneously whether by tectonic uplift or climatic forcing (Molnar et al., 1994; Nicol and Campbell, 2001; Hancock and Anderson, 2002; Bull, 1991). In either case, abandonment most likely occurs due to a propagating knickpoint that migrates upstream through the terrace, and this process can be treated as instantaneous and synchronous as long as the duration of terrace abandonment is short compared with the time since abandonment. In our basic models, base level is held constant, such that beyond the deforming limbs of the fold, successive terraces are superimposed directly on each other. For our purposes, when referring to base-level changes, we refer to regions outside of the actual domain of folding that cause changes in the elevation of the graded profile. Models considering periods of aggradation or incision are presented in the GSA Data Repository (DR1 and DR2).[1]

[1]GSA Data Repository item 2006142, DR1 and DR2 show terrace deformation models with changing base level and DR3 demonstrates how models were created, is available on the Web at http://www.geosociety.org/pubs/ft2006.htm. Requests may also be sent to editing@geosociety.org.

Detachment-style folding commonly occurs in sedimentary sequences with strong mechanical contrasts, such as a thick sandstone sequence above shale or evaporites (Biot, 1964; Currie et al., 1962; Mitra, 2003). Deformation in the competent units may be accomplished by bed-parallel, horizontal, or vertical shear. The easily deformed basal units show various accommodation mechanisms, such as second-order folding and faulting or homogeneous strain (Poblet et al., 1997; Epard and Groshong, 1995). In our models, deformation throughout the fold is assumed to occur by homogeneous bed-parallel shear (flexural slip) in the pregrowth beds. Deformation within the competent units is area-balanced, and all hinges bisect the interlimb angle between the kink bands. The incompetent unit is generally below the graded profile, does not influence the terrace deformation, and may not be area-balanced (Atkinson and Wallace, 2003).

The models assume plane strain and were created with a graphics program (Adobe Illustrator) by rotating and shearing the kink bands that are shown in the models. Each model starts with a pre-existing fold on which terraces are successively emplaced. Specific points on the terrace are pinned to the fold strata and tracked as the deformation progresses, respecting the behavior of the hinges (active, limited, or passive) and the rotation or shear of the limbs. The modeled folds are symmetric, but there would be only geometric, not kinematic, changes if a modest asymmetry to the folds were created. Thus, the key comparisons between the terrace geometries and the bedding orientations presented herein do not change when the limbs are steeper or shallower. The techniques used to create the models are summarized in the GSA Data Repository (DR3; see footnote 1).

Comparison of the model assumptions and field observations is presented in the discussion section. The utility of the models results from two predicted, diagnostic geometries for each fold mechanism: the terrace architecture and the angular relationships between the terraces and the pregrowth strata. These relationships and other observations are described next for (1) angular-hinge limb rotation, (2) hinge migration, (3) a combination of the first two, and (4) curved hinge limb migration.

Limb Rotation

Folds formed by limb rotation maintain a constant limb length while narrowing as the limbs and hinges rotate (Fig. 4A–C; Hardy and Poblet, 1994; Poblet and McClay, 1996; Epard and Groshong, 1995; Mitra, 2003). Such behavior is inferred from geometries of growth strata packages above fault-propagation folds in the

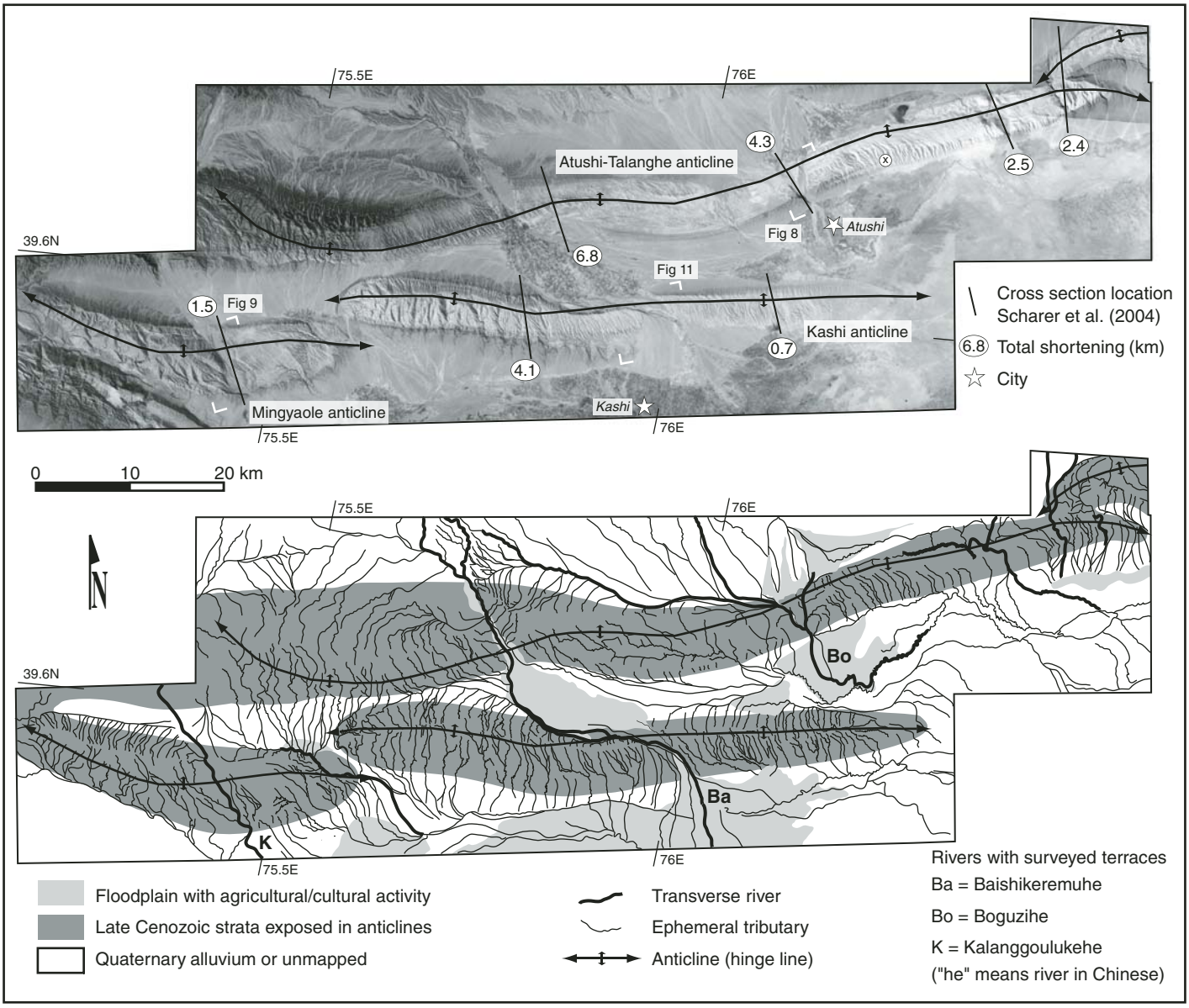

Figure 3. CORONA image and simplified geologic map of Kashi-Atushi fold system. North-directed shortening results in exposed late Cenozoic strata above the Quaternary alluvium. With the exception of the Xiyu Formation, the late Cenozoic sedimentary sequence exposed by the anticlines is easily eroded even by ephemeral streams. The discontinuous darker-gray rim around the anticlines is the conglomeratic and fairly resistant Xiyu Formation. The lateral discontinuity of the Xiyu Formation can be seen northeast of the city of Atushi, where the gray conglomerate pinches out to the east (marked by an X in the CORONA image). Terraces are preserved across three transverse rivers that cut through the anticlines. Regional flow is to the southeast.

Pyrenees (Ford et al., 1997) and the Hikurangi forearc basin (Nicol et al., 2002), and from terrace deformation across the Ventura anticline (Rockwell et al., 1988). In our model, layer-parallel shear accommodates the rotation of the hinges, so that bed length and bed area are maintained. The hinges display limited activity, dependent on the location of the pin line and the thickness of the competent unit. Progressive rotation and shear of fold limbs cause successively emplaced terraces to fan across each limb (Fig. 4C) and produce discordant angles between the terraces and the pregrowth bedding. Layer-parallel shear within the pregrowth beds counteracts the rotation of the terraces, such that the amount of tilt recorded by the terraces will be less than the total rotation of the beds since the terrace was abandoned. (We use the term "tilt" to describe the combined result of rotation and shear on terrace attitudes. Positive tilts are south-dipping, and negative tilts are north-dipping.) In Figure 4B, for example, the pregrowth beds have been rotated 15°, but due to shear, the terrace exhibits only 10° of tilt. Bedding-parallel shear also shortens the terraces within the rotating limb. Changes in base level create distinct changes in the terrace architecture. Uniform incision along the river profile results in an apparent uplift of the older terraces, while aggradation will cause older terraces to terminate into the less-tilted, younger terraces (GSA Data Repository Fig. DR1, see footnote 1).

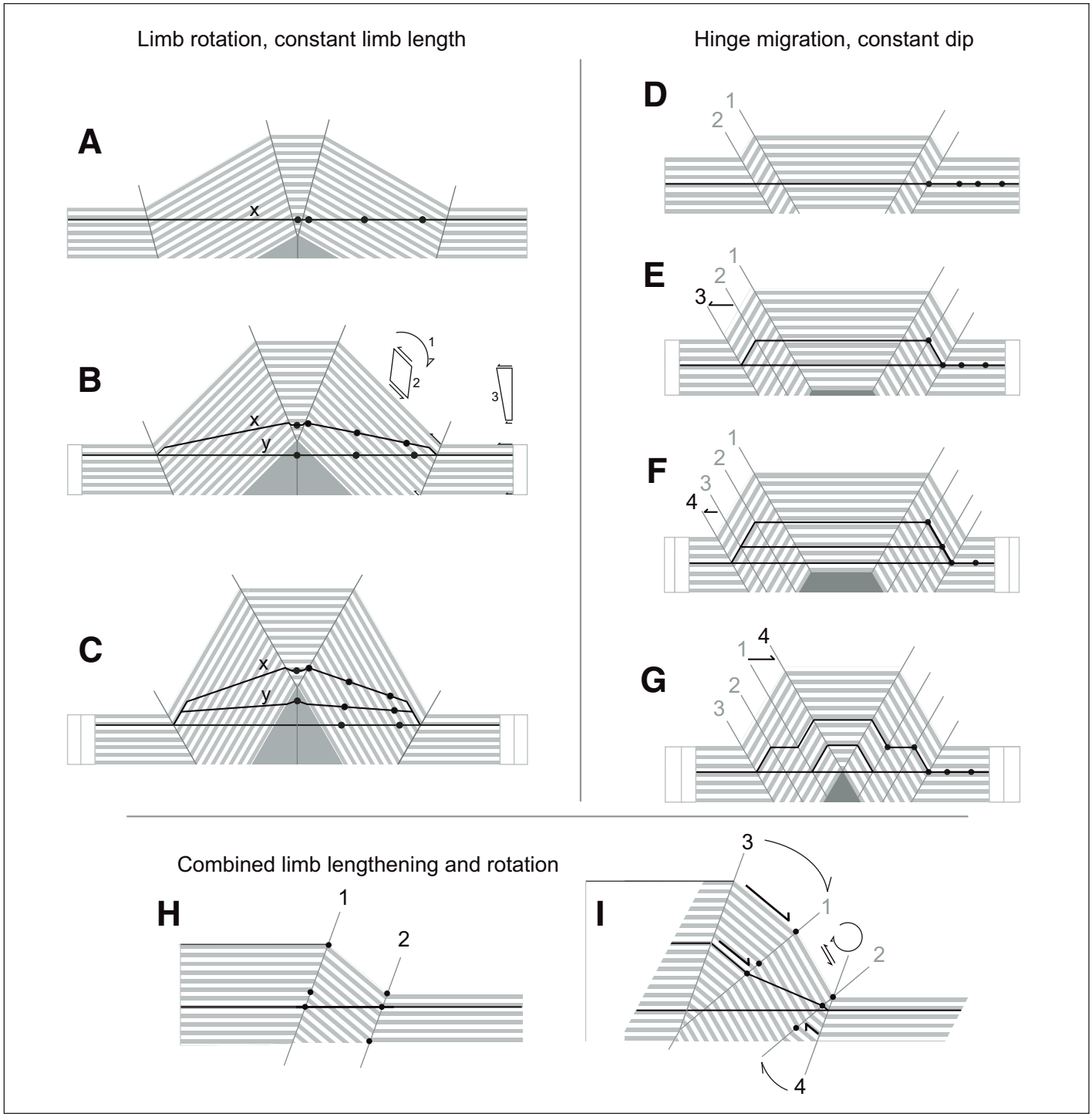
Limb rotation, constant limb length
Hinge migration, constant dip
A
B
C
D
E
F
G
H
I
x
y
1
2
3
4
Combined limb lengthening and rotation

Figure 4. Kinematic models of terrace deformation. The geometry of pregrowth beds is shown by gray and white layers; the terraces are shown by black lines. Boxes on the ends of cross sections reflect actual shortening at each stage. Black circles track points on the terrace through the deformation. In these models, base level is held constant; models considering the effects of aggradation and incision on the terrace geometries are presented in the GSA Data Repository (Figs. DR1 and DR2, see text footnote 1). DR3 (see text footnote 1) shows how the models are generated in Adobe Illustrator. (A–C) Terrace deformation by limb rotation. (A) Pre-existing fold with 120° interlimb angle. (B) Shortening reduces the interlimb angle to 90°, deforming terrace x. This is accommodated by rotation (1) and simple shear (2) to maintain limb length. Because the model is pinned at the fold axis, shear caused by rotation of the hinges is balanced by bedding-parallel shear (3), which pulls material through the hinges. The result is seen in the shoulder of terrace x, where the terrace is parallel to the bedding planes. (C) Additional shortening reduces the interlimb angle to 60°. Deformation within the limb further shears the black circles, and rotates terracey. In the final geometry, the terraces are progressively rotated. The length of terrace that is layer-parallel is dependent on the location of the axis of rotation; in this case, the top of the pregrowth beds was used. (D–G) Deformation of pregrowth strata and terraces by limb lengthening. (D) The fold exists before a terrace is cut across it, with hinges at positions 1 and 2. (E) Hinge 2 migrates to position 3, lengthening the fold limb. Material passes through hinge 3, while hinges 1 and 2 are passive. The terrace and the pregrowth beds follow the same particle path, shown by the black circles moving into and up the limb. (F) A subsequent terrace is cut and similarly deformed. In the final geometry, the terraces are parallel to the anticlinal flats and elevated along much of the crest. Where inclined, the terraces are parallel to the pregrowth strata. (G) Rather than continually growing toward the synclinal axis, this model evolves from (E) by moving hinge 4 toward the anticlinal axis. The fold crest becomes narrower, and the terraces form a ziggurat shape. The stepped geometry of the terrace indicates the sequence and growth direction of the hinges. (H–I) Deformation of a fold limb by combined hinge migration and limb rotation. (H) Pre-existing fold geometry. (I) Axial surfaces 1 and 2 are passive (black circles remain on hinge lines) and rotated, while simple shear (thin arrows) accommodates rotation of the beds within the fold panel to maintain limb thickness. The combination of shear and rotation tilts and stretches the terrace between the passive hinges. Outside of the rotated limb, new material is brought in across active hinges 3 and 4. Within the migrating hinge, material follows the path of the bold arrows, resulting in terraces parallel to pregrowth beds. This configuration can result in considerable shear across the system and is strongly dependent on the choice and location of the passive hinges and points of rotation.

Hinge Migration

Detachment folds can also grow by hinge migration (Mitchell and Woodward, 1988; Poblet and McClay, 1996; Mitra 2003). In this geometry, hinges maintain constant dips, but migrate away from the existing limb (Fig. 4D–G; Fig. DR2, see footnote 1). As the hinge moves laterally, strata move through the hinge, which is therefore considered "active." If the hinge bisects the kink bands, bedding is instantly translated and sheared as it passes through an active hinge, and the strata thickness and bed length are conserved. In the basic model (Fig. 4D–F), the synclinal hinge migrates away from the core of the fold, creating a series of raised, parallel terraces across the center of the fold. On the lengthened limbs, the terraces are superimposed and, importantly, parallel to the dipping pregrowth strata. Alternatively, if previously passive anticlinal hinges become active and migrate toward the core, the deforming domain shrinks, but deformation of the older terraces will be renewed, resulting in a ziggurat geometry (Fig. 4G). In either case, the pregrowth beds and the terraces are parallel where terraces are inclined, and most of the terrace flights will parallel each other. The beds and terraces are not parallel where the fold-limb migration predates the terrace emplacement.

If there is no base-level change, the inclined portions of the terraces will not consist of terrace flights, but will merge into a single, linear feature that is parallel to the dip of the pregrowth strata (Fig. 4F). In concept, a dating transect along the inclined portion of the terraces would result in older ages with increased elevation up the tilted portion. Changes in base level have significant effects on the final terrace geometry. For outward migration of synclinal hinges, incision will be indicated by multiple inclined, but parallel, terraces on the limbs of the fold, creating a *quasi*–self-similar geometry. Uniform aggradation will cause upper, inclined terraces to terminate into the shoulders of lower, horizontal terraces. These model results and those for incision and aggradation during inward migration of anticlinal hinges are presented in the GSA Data Repository (Fig. DR2; see footnote 1).

Combined Limb Rotation and Hinge Migration

Hinge migration and limb rotation are end-member mechanisms of fold growth, both of which may be active successively or contemporaneously during the lifetime of a fold (Dahlstrom, 1990; Poblet et al., 1997; Mitra, 2003, Casas-Sainz et al., 2002; Hardy and Finch, 2005). Figure 4H–I shows how combined hinge migration and limb rotation can deform a horizontal unconformity such as a terrace. The location and activity of the hinges control the overall architecture of the terrace. Importantly, within each kink band, the relationships between the terrace and the pregrowth beds are consistent with the end-member models: parallel where hinge migration occurs and not parallel in the rotated limb.

Curved Hinge

Changes in the width of the hinge can also affect the deformation of pregrowth and growth strata. Suppe et al. (1997) developed models for curved faults and curved hinges. Curved hinges refer to kink bands that are separated by a wide, curved hinge zone rather than a single axial surface that bisects planar kink bands. Notably, a curved hinge causes a set of fanning dips in younger growth strata as the limb lengthens (Fig. 9b in Suppe et al., 1997). The effect on terrace geometries is dependent on the width of the curved surface and the frequency of terrace emplacement (Fig. 5). If the terraces are preserved infrequently and the curved hinges are narrow compared to the overall fold width, the terrace geometry will appear as in Figure 4D–F, but with curved, rather than sharp, shoulders and basal transitions if the terrace is emplaced before the stationary hinge is established. Either way, the effect is minor relative to the length of a terrace. Changes that are more significant occur if the curved hinge is wide. In Figure 5B, the curved hinge has translated a distance equivalent to the width of the limb. Progressive migration of the active hinge and terrace emplacement create fanning terraces coincident with the migrating hinge. The core of the fold is marked by the parallel horizontal terraces characteristic of hinge migration.

The width of the active hinge and the timing of the terrace emplacement control the final terrace and pregrowth geometries. Nonetheless,

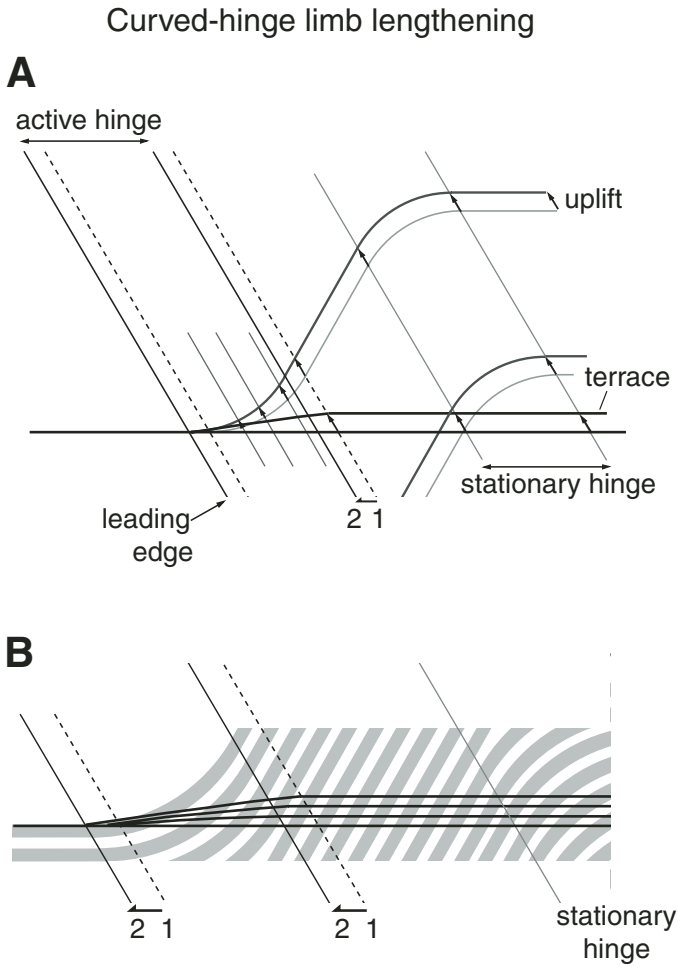

Figure 5. Deformation of pregrowth strata and terraces by limb lengthening with a curved hinge. (A) Kink bands are separated by a wide, curved hinge in which material is deformed along similar circles. Within the active hinge, material moves along particle paths that are parallel to the hinge axes (thin gray lines). Beds or terraces present within an active hinge are bent into a curve and then raised uniformly when the hinge has passed, as shown by small black arrows (modified from Suppe et al., 1997). (B) In this enlargement, the width of the curved hinge is expanded and the rate of terrace emplacement increased. As the active hinge migrates from position 1 to position 2, pregrowth beds (thick gray lines) are lifted along particle paths parallel to the hinges. All material to the right of the active hinge is raised uniformly. Within the migrating hinge, the uplift reduces to zero at the leading edge (left). Terraces developed along a stationary river profile (black lines) are also lifted, in increments consistent with the structural development. Like the beds, everything to the right of the active hinge is raised similarly, resulting in parallel terrace treads. The uplift reduces to zero at the leading edge of the active hinge, so that incremental uplift results in fanning terrace treads where the active hinge has migrated since terrace emplacement.

general observations can be drawn. Across the core and most of the limbs, the terrace treads remain parallel, but are discordant with the beds on which they are emplaced. The terraces fan within a narrow triangle. The width of the triangle indicates the width of the zone across which the active curved hinge has moved. Only at the outer edges of the folds do the terraces and beds have a similar slope, because at this location, both the bed and terrace begin with a horizontal orientation and are deformed synchronously.

KASHI-ATUSHI FOLD SYSTEM

The Kashi-Atushi fold system includes three east-west–trending, 60–100-km-long anticlines (Fig. 3). Semiarid climate inhibits vegetative cover and provides exceptional exposure. The folds are tight to box-like and reveal Neogene through Pleistocene strata deposited in the Kashi foredeep at the southern margin of the Tian Shan. The outer layers of the anticlines consist of the Xiyu Formation, a moderately well-indurated conglomerate with significant lateral thickness variations (Fig. 3). The conglomerate interfingers into a generally fining-down sequence of sandstones, mudstones, siltstones, and gypsum, which are well bedded but easily eroded (Fig. 6). The anticlines are strongly incised and exhibit only ~500 m of topography where cross sections indicate 2–4 km of structural relief developed. Total reconstructed shortening decreases toward the east, ranging from ~7 to 1 km over the last 1–3 m.y. (Fig. 3). Geodetic studies record regional shortening (Holt et al., 2000; Reigber et al., 2001) that is relaxed by small to large earthquakes (CSB, 1997) and possibly by aseismic deformation as well. Scharer et al. (2004) and Chen et al. (2002) presented a detailed discussion of the fold stratigraphy, structure, and ages of the folds.

The major transverse rivers are fed by glacial melt from the hinterland and local and regional storms. Smaller tributaries and streams are ephemeral and characterized by flash floods during local storms. We address three of the five rivers that cross the anticlines and ultimately drain into the Tarim Basin (Fig. 3). The Kalanggoulukehe and the Boguzihe ("he" indicates river in Chinese) have cut wide valleys where they enter the anticlines, but exit through narrow gaps in the Xiyu Formation. The Baishikeremuhe is similarly broad at the entrance, but shows eastward migration across the southern limb. Within the water gaps, the valleys are broad, exhibiting transitional to braided channel patterns. Outside of the water gaps, the floodplains are braided. Modern longitudinal river profiles have slopes from 0.6° to 1.1° through the water gaps.

Terrace Characteristics

Terraces across the Atushi-Talanghe, Mingyaole, and Kashi anticlines are strath terraces (sensu Pazzaglia and Brandon, 2001), covered by only 0.5–2 m of gravel with rare sand lenses. Clasts on the surface are tightly packed and show textural evidence of eolian erosion. The treads are generally planar and show minor erosion except close to gullies that cut through the underlying strata (Fig. 7). Where steep gullies erode into the terraces and provide good exposure, and where topographic surveying of both was possible, the tread and the strath appear essentially parallel. Surveys were conducted with a laser ranging theodolite (total station) in 2000 and 2003 and were generally restricted to

one side of the valley. Most of the survey paths were linear and parallel to the terrace gradient. The slope of these terraces was determined by least squares methods. Where the tilt of a terrace was subtle (primarily on small remnants at the core of the Kashi anticline), longitudinal and transverse profiles were surveyed, and a plane was fit to the data by linear regression methods. These planes had a maximum dip direction within 10° of the cross-section orientation. We avoided surveying areas with obvious young colluvium deposited from the riser above the terrace, as well as outer terrace edges where the gravel tread appeared to be raveling off the strath. The survey data are projected onto a vertical plane oriented perpendicular to the strike of the anticline, so the dips presented are apparent dips.

Data collected in 2000 have vertical surveying errors of ≤10 cm, which accrued during individual resections. Along individual terrace sections, however, the errors in the tilts of the terrace surfaces should be negligible because all but four terrace sections were surveyed from single base stations. Therefore, resections required to access separate terrace surfaces along the water gaps could contribute up to one meter errors in the height of individual terraces relative to each other but not affect the absolute tilt. In the worst case, the resection errors would be additive, resulting in errors of ±0.4° for the Boguzihe and Kalanggoulukehe profiles (which include 4–5 resections each). Resectioning during the 2003 survey of the Kashi profile accrued random errors of <3 mm during each of eight resections.

Boguzihe Water Gap

Fluvial terraces are preserved at the core and on much of the southern limb of the Talanghe anticline at the Boguzihe water gap (Fig. 8). The water gap was created by two primary rivers, the West and East Boguzihe. In between the two rivers, a triangle-shaped island of Neogene strata and terraces has been isolated between the canyons. It is unclear if the highest terraces, T7 and T8, were cut by the western or eastern channel, whereas the lower terraces certainly result from lateral planation by the West Boguzihe.

In cross section (Fig. 8C), the most-extensive terrace treads are preserved on the overturned to steeply dipping panels of the southern limb. These terraces display a progressive increase in tilt with age and are nowhere parallel to the bedrock dips. The surfaces are planar and not kinked, indicating the axial surfaces have been passive since the terraces were emplaced. The tilt between the younger terraces is modest (0.4° between T1b and T6) but increases to ~0.9° between T6 and the oldest preserved terrace, T8.

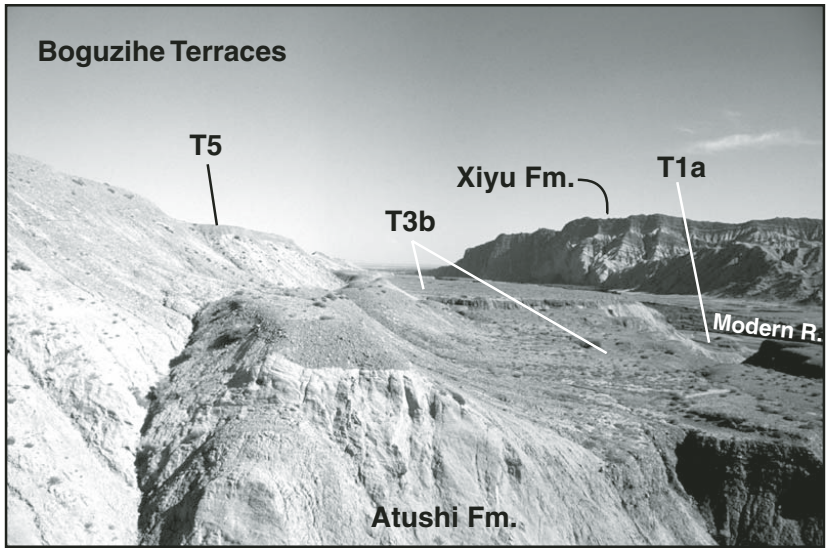

Figure 6. Photograph of terraces on the southern limb of the Atushi-Talanghe anticline. The cliff in the background is created by the capping conglomeratic Xiyu Formation, which interfingers below with the sandstone and mudstone Atushi Formation. Terrace T3b is broader and more continuous than other terraces in this water gap. View is to the south and located on Figure 8; the vertical separation from T3b to T5 is ~10 m.

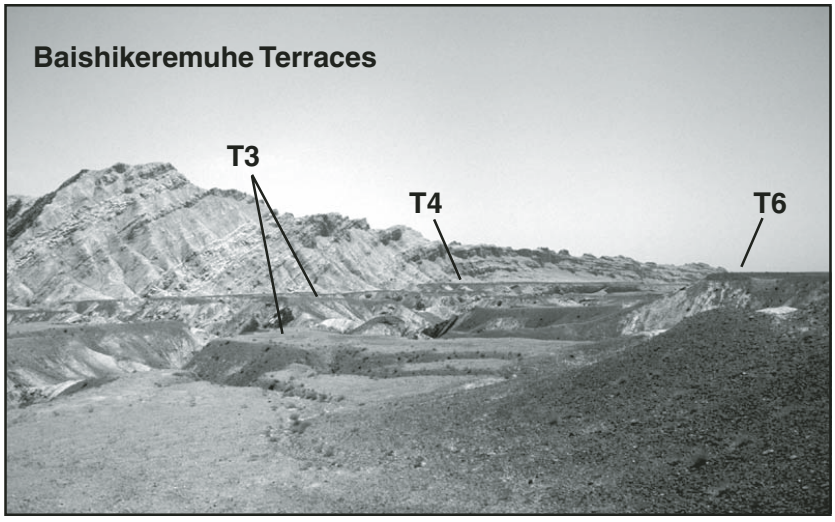

Figure 7. Photograph of terraces across the core of the Kashi anticline. Steep gullies cut through the terraces and reveal thickness of the gravel cover. Away from the gullies, the treads are fairly planar and show little fluvial erosion. View is to the east and located on Figure 11. The vertical distance from T3 to T6 is ~10 m.

When projected to the south, the oldest terrace surfaces would intersect the surfaces of T6 and younger (Fig. 8C). Short terrace segments on the northern flank of the fold have the greatest tilts (–2.3° relative to the Boguzihe) documented at this water gap. The oldest surveyed terrace on the northern side (T2c–T3a) is faulted, with a vertical separation of 4.1–5.7 m.

Kalanggoulukehe Water Gap

At the Kalanggoulukehe, fluvial terraces are preserved across most of the Mingyaole anticline (Fig. 9). The terrace profiles are generally straight where they cross hinges, are nowhere parallel to the dips of the Neogene strata, and display tilt directions consistent with the dip directions of the beds. Terrace T7j is the only

Figure 8. Map and profiles of Boguzihe fluvial terraces on the Atushi-Talanghe anticline. (A) Geologic cross section of the Talanghe anticline (from Scharer et al., 2004). Above the modern topography, the structure lines are dotted and the Xiyu Formation is lighter gray. (B) Aerial photograph annotated with map of surveyed terraces, major structural features, and formations. With the exception of T7 and T8, the surveyed terraces are related to the West Boguzihe River. The northern half of the anticline is largely eroded by the Boguzihe. (C) Composite cross section of terrace profiles and bedding dips. Below the river profile, the axial surfaces and bedding dips (gray bands) are displayed with no vertical exaggeration. Above the river, everything is shown with a 10× vertical exaggeration, (resulting in the bend in the axial surfaces as they cross from 1× to 10× vertical exaggeration across the river profile). Thin black lines projected from terrace surveys illustrate rotation on the southern limb. The absolute dip of the beds and tilt of the terraces are indicated with bold and italicized number, respectively.

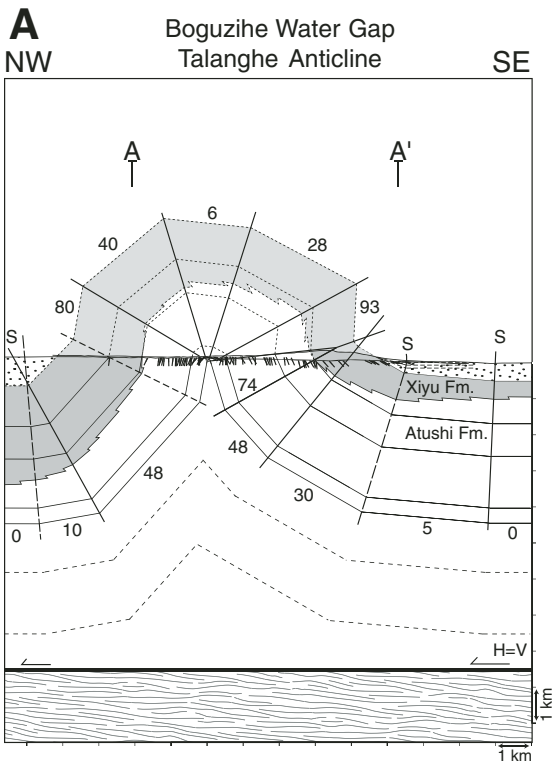

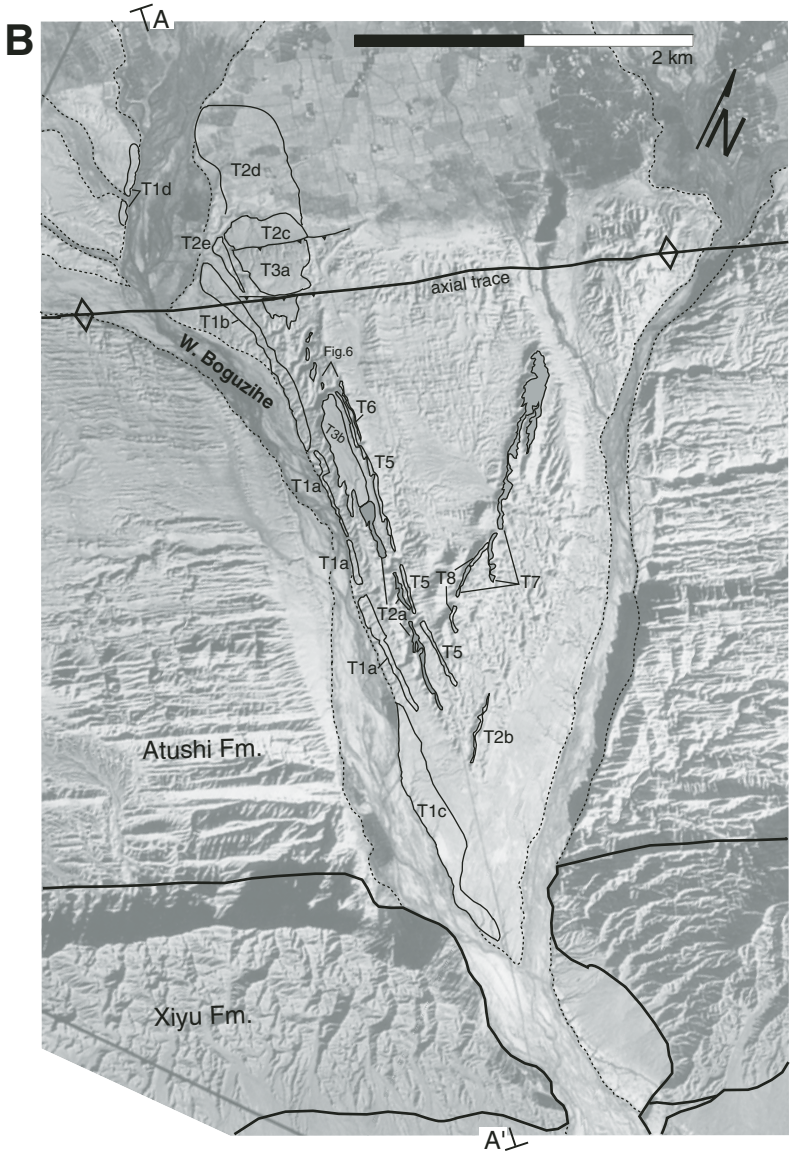

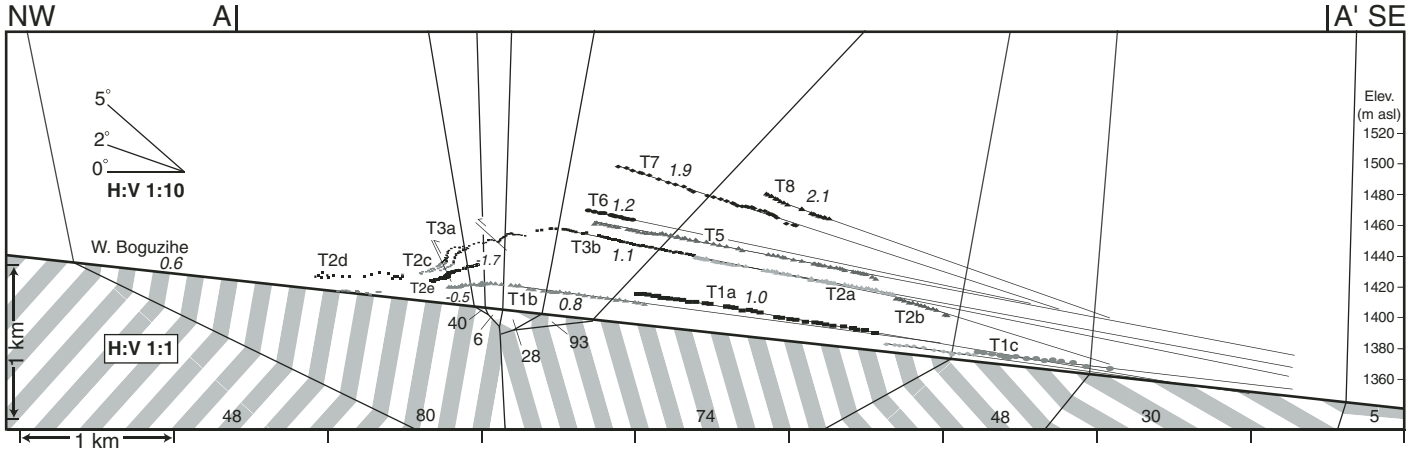

terrace that is not planar; instead, it is gently curved where it crosses a hinge close to the core of the fold. In cross section, two obvious sets of terraces are vertically separated by 50–100 m (Fig. 10). In comparison to the modern fluvial slope across the anticline (1.0°), the younger set of terraces shows a minor relative rotation of >0.3° on both limbs. On the southern limb, terrace T7a is parallel to the modern river. Terrace T7 b–h is a continuous surface, but is not planar. Rather, the top is tiered, broken by five small, down-to-the-south steps (Fig. 9). We were unable to survey the strath of T7, so this morphology could result from accommodation faulting in the underlying strata, or more likely, lateral migration of the river before the terrace was abandoned. Individually, the T7b–h terraces range in dip from 0.3° to 1.3° greater than the modern channel.

The greatest terrace dips documented in this fold system are from the northern limb: T7j, located on bedrock that dips 10° and has been tilted –6.2° relative to the modern river gradient (Fig. 10). Terrace T9b consists of a suite of treads and risers beveled into the Xiyu Formation. Compared to the 1° southward slope of the modern river, the terraces tilt –6° to –8.7° to the north. Significant tilts (–6.0°) in the upper, northern terraces suggest that segments on this limb were deformed after the upper terrace set was abandoned, whereas very minor rotation (–0.2°) has occurred since T4 and T5 were abandoned (Fig. 9). Additionally, it appears that deformation was focused on the northern limb, or at least segments of the northern limb. In contrast, on the southern limb, T7a and the modern river are parallel, but vertically offset by ~70 m. A scarp at the axis separating the 58° and 34° kink bands may reflect incision, reverse faulting, or a fold scarp. In our models, a fold scarp in this location can be produced by synclinal migration of an active hinge (Fig. 4D–F), or limited activity across a hinge that is accommodating limb rotation (Fig. 4B–C). Parallelism between T7a and the modern river suggests rotation since T7a has been minimal, and hinge migration is the more likely mechanism.

Baishikeremuhe Water Gap

The Baishikeremuhe cuts obliquely through the center of the Kashi anticline, resulting in only short stretches of terraces preserved subperpendicular to the trend of the fold (Fig. 11). The position and elevation of the terraces with respect to the Baishikeremuhe indicate that the river has migrated to the west since these terraces were abandoned (Fig. 3). The present course of the Baishikeremuhe is south of the highest terraces, T5 and T6. The presence of terraces T4 through T1, to the north but lower in elevation, suggests that the Baishikeremuhe diverged to the north around T5/T6 in the past and abandoned the northern passage after T1 was beveled. As a reference gradient, we surveyed the small ephemeral drainage that cuts through the terraces (dotted line, Fig. 11B), assuming that it is a relict canyon of the Baishikeremuhe. The slope (1.1°) is equivalent to the slope measured at Kalanggoulukehe, and provides our best estimate for the paleoslope of the Baishikeremuhe. T7 is a long terrace on the south side of the Baishikeremuhe that also has a slope of 1.1°.

When projected onto a vertical profile, terraces T1e, T2a, T2b, and T3a on the northern limb show decreased tilts with age (Fig. 11C). This apparent contradiction of model expectations is explained by two features: the structure and the plan-view arrangement of the terraces. First, the eastward plunge of the Kashi anticline is also seen in the dip direction of the terraces (N2°E), which has been projected onto a N7°W cross-section line. Second, the terraces are projected along strike for ~1 km, and their dip may reflect changes in deformation down plunge, for example, increased rotation to the east.

As observed in the other water gaps, the terraces continue flat across hinges in the limbs and are steepest on the northern limb (Figs. 11 and 12). The oldest terraces, T5 and T6, are laterally extensive and have a modest relative tilt of –0.3° to the north. About 20 m below, T4a and T4b are also gently dipping and do not show evidence of deformation across the anticlinal core. T3a is gently folded, but the axis of the terrace fold is north of the axial trace of the anticline; T3 dips 3.3° to the south, on Atushi Formation strata dipping ~0° to the north. No faults were observed in that area, but the antithetic dips suggest complicated deformation in the core of the Kashi fold.

DISCUSSION

Kinematic History

It would be erroneous to directly compare the kinematic models, which use idealized fold limbs consisting of single kink bands, with the Kashi-Atushi folds, which have many kink bands, both narrow and wide (Figs. 8A, 9A, and 11A). To unravel the kinematics of folding, we compare the general predictions of the models to observations of the terrace and bedrock deformation in the Kashi-Atushi fold system. The strata thicknesses and lithologies are similar at each anticline, which suggests the mechanical response to compression should be similar at each transect (Hardy and Finch, 2005), and we can use observations from all of the transects to constrain a general kinematic model (Fig. 13). Before considering the terrace geometries, however, it is appropriate to summarize observations of the Kashi-Atushi folds along strike. All of the anticlines have a similar shape composed of a tightly folded core developed over shallowly dipping outer flanks (Figs. 8A, 9A, and 11A). In general, total shortening reduces to the east both regionally and within each anticline (Fig. 3). Seismic surveys indicate fold widths do not change significantly along strike despite the five-fold differences in total shortening (Scharer et al., 2004). Transects with greater total shortening exhibit longer steeply dipping kink bands and greater fold amplitudes. Growth strata on the outer edges of these folds are fanning, a geometry consistent with limb rotation (Poblet et al., 1997) or curved hinge-zone migration (Suppe et al., 1997).

Our kinematic model combines these geometric structural observations with kinematic inferences developed from the terrace geometries. There are three basic observations that can be made at each of the water gaps. First, in each profile, the terrace treads are discordant with the beds into which they were beveled, but the dip directions of the terrace and underlying strata are usually consistent. Second, the terrace treads exhibit increased dips with age. Third, terrace elevations are highest in the core and decrease toward the limbs. These observations indicate that the core of the fold is not raised as a uniform block as predicted by hinge migration; instead, it is raised by progressive rotation of the limbs (Fig. 13). Furthermore, many terrace profiles show no inflection, indicating that the hinges the terrace profiles cross have been passive since the terrace was abandoned. This implies that many of the hinges across these folds were established earlier in the history of the fold, but have not accommodated shear over the last ~20–100 k.y. (Van der Woerd et al., 2001).

Extensive preserved terraces on the southern limb of the Talanghe anticline provide additional constraints on the evolution of the folds. When extrapolated to the south, the older terrace profiles (T7 and T8) on the southern limb of the Talanghe anticline (Fig. 8) intersect with projections of terraces younger than T6. This geometry is similar to the model predictions for aggradation during limb rotation (GSA Data Repository Fig. DR1; see footnote 1). However, those predictions also require that the lower terraces must be fill terraces, and this contradicts field observations of thin gravel above the strath of T1 through T6, which indicates that these are not fill terraces (Fig. 7). An alternative mechanism to produce truncating terrace profiles is to jump the location of the hinge outward over time. We propose that T7 and T8 were emplaced

Figure 9. Map and profiles of Kalanggoulukehe fluvial terraces across the Mingyaole anticline. Conventions for A, B, and C are as in Figure 8. Terraces are preserved across the entire anticline at two primary elevations, ~20 m and ~100 m above the modern river. The tilt direction of the terraces is consistent with the dip direction of the pregrowth beds, and the crest of the elevated terraces is coincident with the center of the anticline. Note that the terraces are kinked only at the core of the fold.

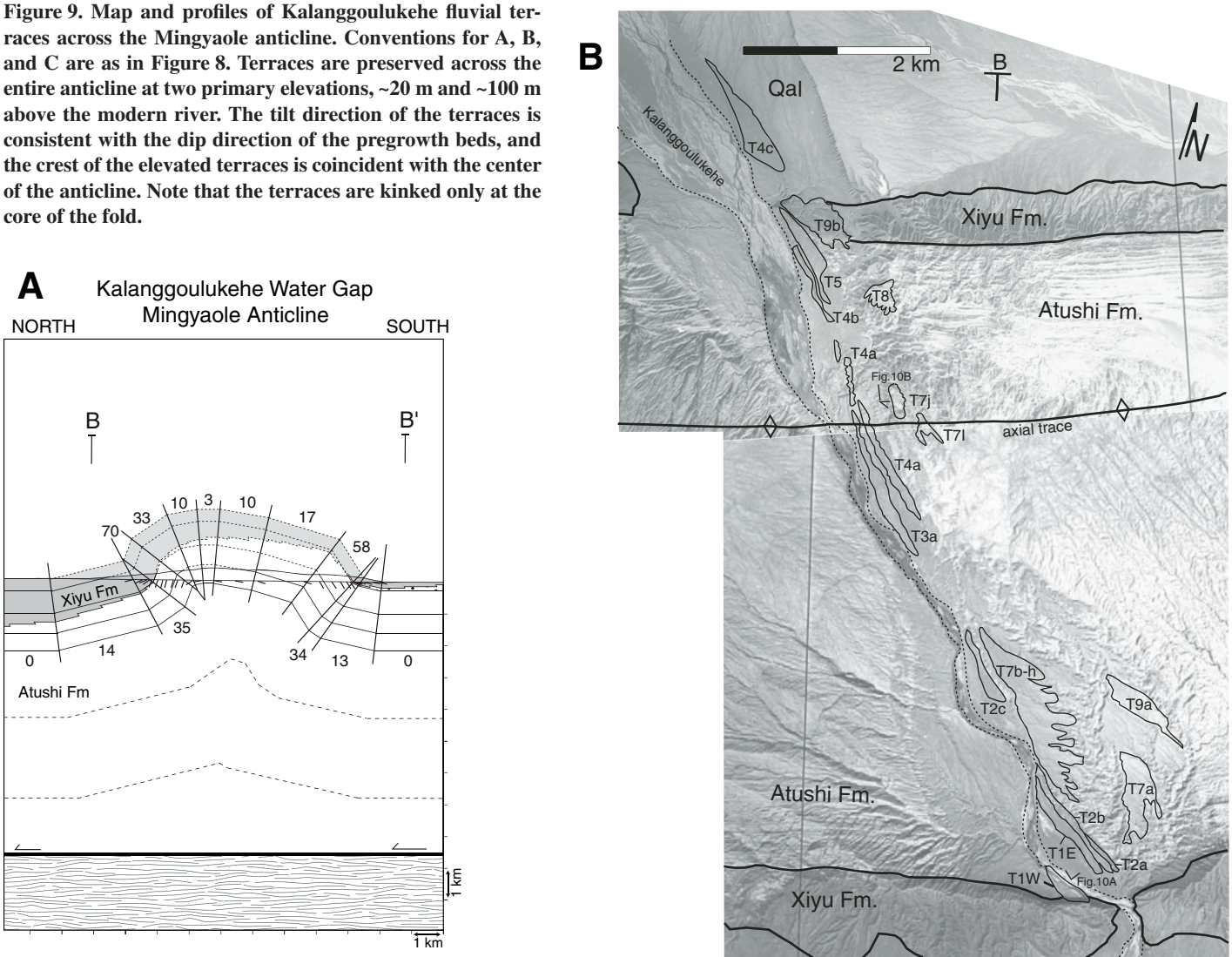

and deformed when a major axis of rotation was approximately located at the hinge separating the 48° and 30° kink bands (Fig. 8). Following this, the major axis of rotation shifted to the current, more southerly, location. In further support of this mechanism, none of the terraces shows inflection across the hinges, suggesting that the entire southern limb has behaved as a single block since T6 was abandoned.

On the southern limb of the Mingyaole transect, progressive flattening of terrace T7a–h can also be created by episodically shifting the limited activity hinge outward until T7a was abandoned. Time steps *t*2 to *t*3 in the kinematic model represent the outward shift of the rotation hinge and show how this increases the fold amplitude over time (Fig. 13).

A different mechanism is suggested by the terraces located proximal but on the northern side of the core of the folds. Here, all of the water gaps have short, relatively steeply dipping terrace surfaces: at the Kalanggoulukehe water gap, terrace T7j has rotated –6.2° relative to the modern river gradient. At the Boguzihe, terraces T3a and T2e both show a dip of –2.3° relative to the modern river gradient. Terraces T1e and T2a at the Baishikeremuhe dip –5.3° and –3.4°, respectively. Each of these terraces is short, and some cross hinges. For each, extrapolation of the terrace profile indicates a deforming section that is significantly narrower than the width of the fold limb. Unlike the gentle terrace tilts across the southern limb of the Atushi and Mingyaole anticlines, which appear to involve the entire limb, these northern deformed panels are proximal to the core of the fold. Short-wavelength deformation at this location is coincident with the presence of small, accommodation faults at Boguzihe, and the modest but consistently northward vergence of the anticlines. To reproduce this observation in the kinematic model, we produced a narrow band of shear to the north of the core by rotating the northern limb a bit less than the southern limb (Fig. 13).

In summary, we used increases in total shortening as a proxy for fold age in combination with evidence from the shape of the anticlines, growth strata, and terraces to develop a kinematic history of the Kashi-Atushi fold system (Fig. 13). Similarity of the fold forms along strike suggests that the general shape of the fold is developed early and is subsequently amplified throughout the history of the fold, but not in a purely self-similar style. Continued shortening is accommodated, in part, by increasing the length of steeply dipping kink bands by episodically shifting the limited activity hinges outward with time. This is consistent with the observed terrace geometries and the increase in fold amplitude with continued shortening. Planar, rotated terraces indicate more recent folding is accommodated by block rotation of the limbs. The widths of the folds are maintained by translation of pregrowth bedding across the outermost hinges and up into the shallowly dipping flanks, which also preserve growth strata on the outer flanks of the fold (Scharer et al., 2004).

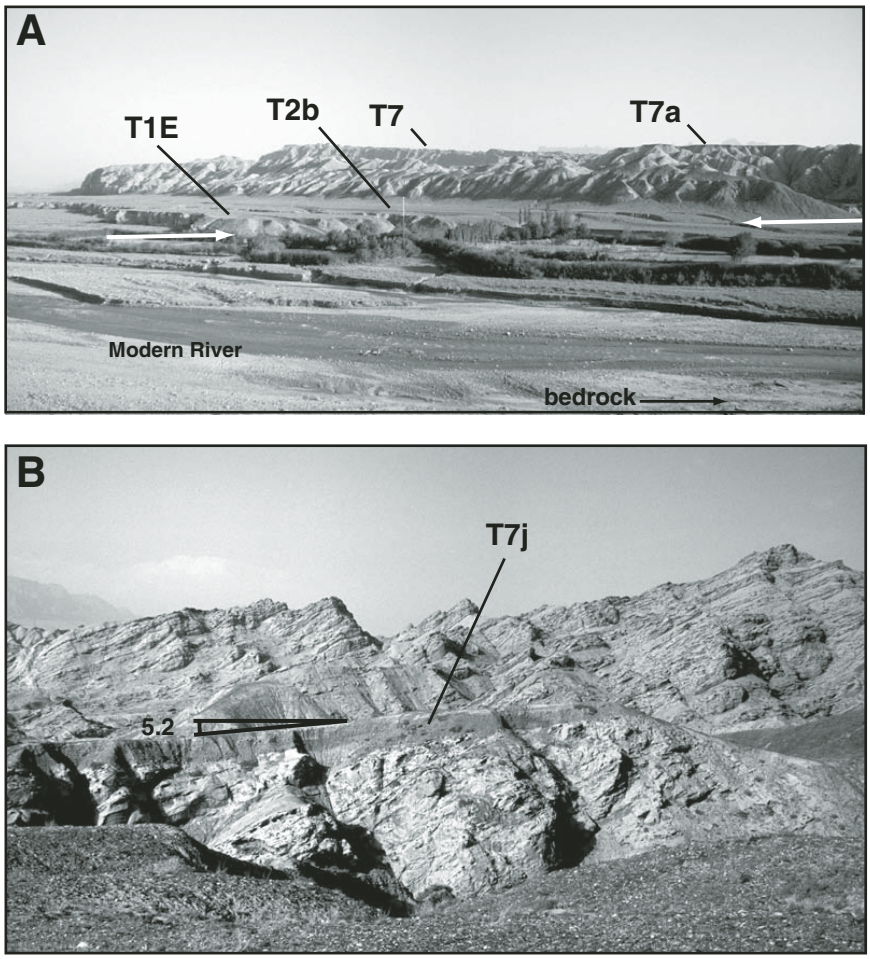

Figure 10. Photographs of terraces on the Mingyaole anticline. (A) A flight of terraces on the southern limb is visually dominated by T7 and T1/T2. A scarp offsets T2b by 4–5 m (between white arrows, also see Fig. 9C), and could result from hinge migration rather than faulting. South-dipping Atushi Formation strata are exposed in the modern riverbed. View is to the north-northwest, located on Figure 9, and scale is provided by trees partially obscuring scarp. (B) Photograph of terrace T7j, which tilts –5.2° to the north (the tilt relative to the modern stream is –6.2). The Atushi Formation below dips 10° to the north. The gravel package is ~1 m thick.

Paleogradient

Our interpretation of the terrace deformation requires that the river's long profile maintains a nearly constant slope through time. For example, we use the progressive decrease in terrace slope for the succession of old to young terraces on the south flank of the Boguzihe water gap as evidence for limb rotation. If, instead, the river gradient were systematically decreasing over this time, limb rotation might be unnecessary to explain the changes in terrace slopes (but it would not explain back-tilted terraces on the northern limb). Short-term (hundreds of years) changes in discharge and sediment yield in a river can be accommodated by local changes in the river planform, such as by variations in sinuosity (Schumm et al., 1987). In contrast, long-term changes (thousands of years), such as those induced by climate change or a change in the lithology into which a river is cut, can create catchment-scale changes in the profile and shape of a valley floor (Lavé and Avouac, 2000; Pazzaglia and Brandon, 2001; Poisson and Avouac, 2004). The young, uppermost layer of Xiyu Formation conglomerate was eroded early in

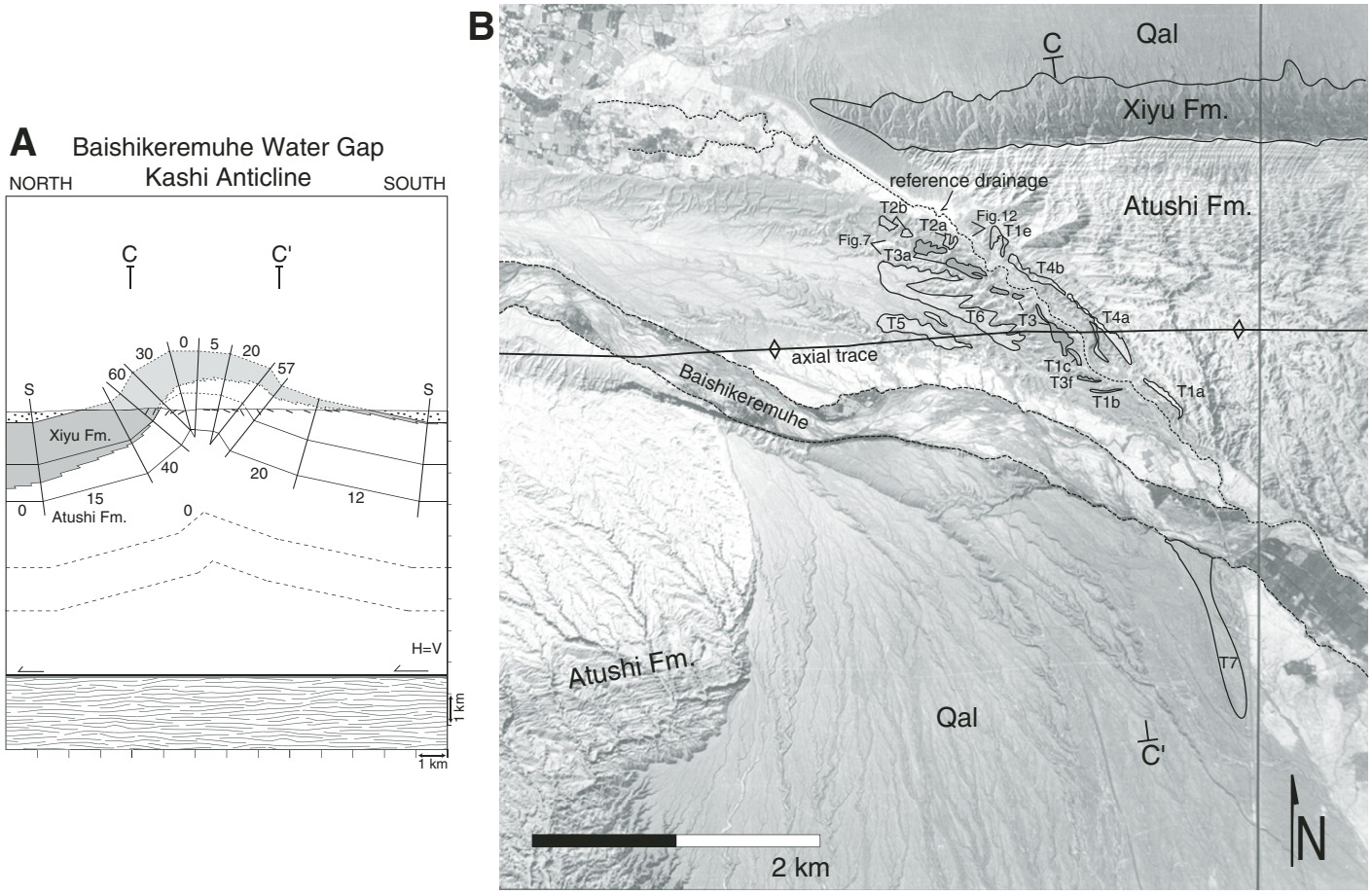

Figure 11. Map and profiles of Baishikeremuhe fluvial terraces across the Kashi anticline. The small tributary (dashed line) that flows through the terraces, not the Baishikeremuhe, was used for the reference datum. Conventions for A, B, and C are as in Figure 8. Terraces on the north side of the Kashi anticline appear to decrease in tilt with age. This results from projection of plunging surfaces onto the cross-section line. The crest of the elevated terraces is located ~400 m north of the center of the anticline.

the life of the fold, and since then the rivers have flowed over soft and readily eroded sedimentary layers for most of the duration of fold growth; therefore, a change in lithology is unlikely to be an important controlling factor.

We cannot determine independently the paleogradient of the rivers and, therefore, must rely on several observations that suggest river profiles across the folds have remained relatively constant. First, if we were to assume that gradients were previously steeper, such as the slopes observed on the highest, oldest terraces at Boguzihe, and we were to project this gradient (~2°) toward the hinterland, the reconstructed river would be nearly 1 km above its present profile. No evidence in the hinterland supports paleorivers near this elevation in the recent past. In fact, terraces in piggyback basins within the hinterland thrust sheets in the more northerly parts of the catchment are typically a few tens of meters above the modern river, similar to analogous terraces on the outer limbs of the folds studied here. If paleogradients were significantly steeper than today, these low terraces in the hinterland would have to be much younger than those that appear correlative with them in our southern study area. Weathering and desert pavement development look similar on the 5–25-m-high terraces in both the foreland and the hinterland. Second, terraces on the northern limbs of the folds are north dipping, opposite the river gradient, which indicates that structural deformation is intrinsic to the attitude of the terraces. Finally, field observations suggest that aggradation is not active, either. At the southern end of the Kalanggoulukehe water gap, dipping Neogene strata are visible in the active channel (Fig. 10), and no fill terraces are preserved in this system. In sum, we found no evidence that observed changes in terrace gradients are likely the result of a long-term change in the overall gradient of the river.

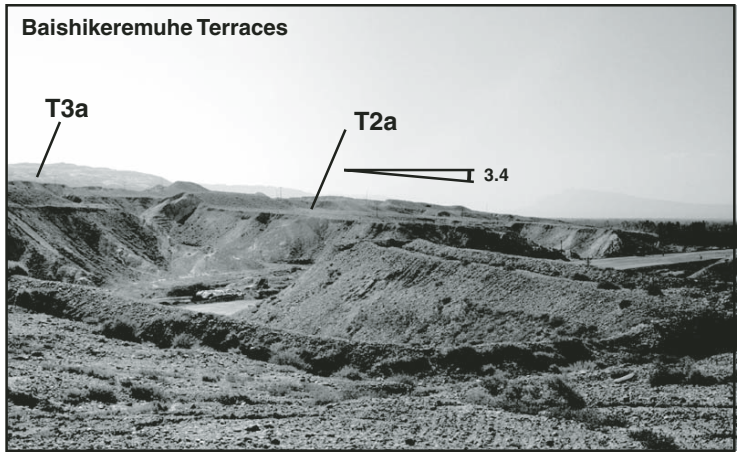

Figure 12. Photograph of terraces on the Kashi anticline. The lower terrace remnants on the northern limb show the greatest dip across this anticline. Terrace T2a is ~20 m above the reference drainage in the center of the image.

Uplift, Shortening, and Incision

If the long-profile gradient of the river remains relatively constant through time, does differential uplift or incision control the observed height of the terraces above the modern river? If incision due to base-level lowering controls terrace heights, lowering the river profile should produce terraces that are uniformly separated from each other outside the deformed region. Even if climatically induced changes in gradients were to have occurred, such as would be expected with increased sediment flux and a steeper long profile, the relative heights of terraces at any position along a river's gradient should remain consistent. Instead, we clearly observe terraces merging or diverging within the folds themselves, and correlative terraces are typically not preserved in adjoining synclines. The highest terraces between the studied folds or downstream of them are typically <5 to 10 m above the modern channel. This sets an upper limit on the amount of regional incision that might affect modern terrace heights. Consequently, nearly all of the observed terrace heights must be attributable to differential uplift.

Using estimates of shortening rates (Scharer et al., 2004) and the relationship between shortening and uplift during detachment folding (Fig. 1), we can estimate the age of the highest terraces under the assumption that differential uplift alone controls the elevation of the terraces. If hinge migration dominates, uplift is slightly less than shortening. If limb rotation dominates, uplift is greatest at the early stages of folding, where it can exceed three times the shortening rate. As limbs become progressively steeper, shortening rates approach differential uplift rates. At the studied water gaps, excess area calculations indicate that the Kashi-Atushi folds have accommodated 1.5–4.3 km of shortening over the past 1–2 m.y. (Scharer et al., 2004). The interlimb angles are tight to isoclinal, which indicate shortening and differential terrace uplift rates should be nearly equivalent. Estimated ages for the highest terrace at each fold, therefore, can be calculated, assuming that shortening and differential uplift are equivalent, that shortening rates have been constant through time, and that fold growth initiated ca. 1.2 Ma (Chen et al., 2002). In this scenario, the resultant minimum ages of the highest terraces range from ca. 12 ka to 24 ka to 85 ka for the Kashi, Atushi, and Mingyaole folds, respectively. Overall, it is likely that the terraces were created and abandoned in relatively brief climatically controlled intervals (Hancock and Anderson, 2002; Molnar et al., 1994; Pan et al., 2003, Thompson et al., 2002). Here we conclude that their subsequent positions above regional base level are largely due to differential tectonic uplift.

CONCLUSIONS

Where compression is accommodated by surface folding rather than discrete faulting, the evolution of deformation may include different shortening mechanisms and varying relationships between uplift and shortening. Successive kinematic markers that are progressively deformed are needed to unravel these relationships and illuminate how they have changed over time. Fluvial terraces that are preserved across growing anticlines provide a unique record that can further understanding of the kinematics of fault-related fold growth. Because terraces are generally superimposed on older folded strata, they record the deformation mechanism within the fold. Furthermore, they can provide both an integrated picture of the total deformation, as well as snapshots of deformed terraces that capture stepwise (or incremental) deformation of the fold. In contrast to growth strata, terraces preserve kinematic information in regions where uplift outpaces subsidence. Terraces are also typically preserved across the cores of folds—a region where growth strata are commonly missing.

We present kinematic models for four types of detachment folds and fluvial terraces successively emplaced across them. The kinematic history is revealed in the terrace architecture and the angular relationship between the terraces and the strata dips for each model: (1) Deformation by limb rotation is marked by progressively

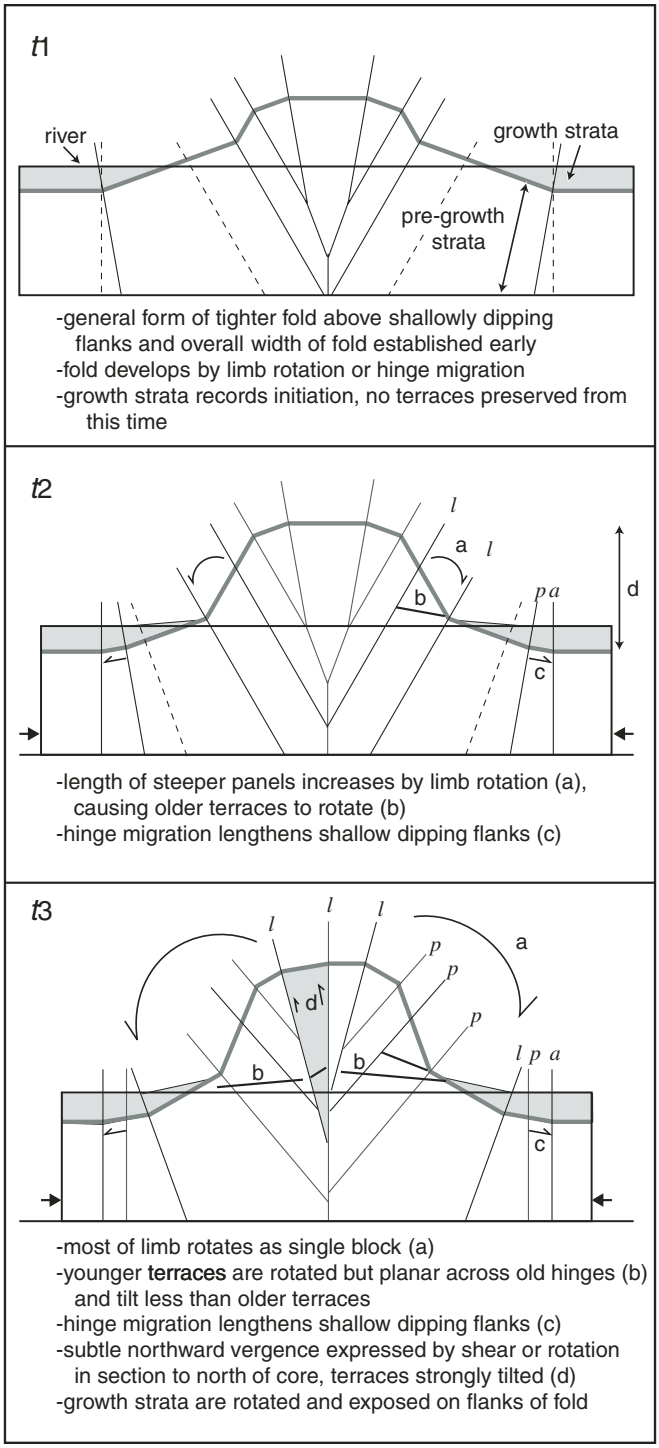

Figure 13. Cartoon of the kinematic model inferred for the Kashi-Atushi anticlines at three successive stages (t_1–t_3). As in Figure 4, active, limited, and passive hinges are designated with *a*, *l*, and *p*, respectively, and the migration of hinges and/or rotation of limbs are shown with bold arrows. No terraces are preserved until later stages, so we infer the early form of the folds would be consistent with observations along strike in which transects with less shortening have small amplitudes and short panels of steeply dipping beds (Scharer et al., 2004). In the second frame (t_2), the fold amplitude is increased as sections of the uplifted core from t_1 undergo limb rotation. By t_3, the youngest terraces are longer and gently tilted, which requires that hinges within the limb are passive and most of each limb rotates as a block. Outward migration of the outermost hinges preserves the long, gently dipping flanks of the fold observed in seismic-reflection lines.

tilted terraces across the limbs. (2) Migration of an angular hinge results in parallel, uplifted terraces in the core and dipping terraces along the fold's flanks, where they are largely parallel to the dip of pregrowth strata. (3) When limb rotation and hinge migration are combined, the terrace architecture is consistent with the kinematics acting on individual kink bands. (4) The geometric result of limb lengthening by migration of a curved hinge is dependent on the width of the curved hinge. If the hinge is wide and terrace abandonment is frequent compared to the hinge migration rate, fanning terraces result. These models provide a new and underutilized framework for dissecting the incremental growth of a fold.

The model predictions are compared to fluvial terrace flights preserved in three water gaps in the Kashi-Atushi fold system. The anticlines are characterized by tight cores that rise above gently dipping outer flanks. The terrace profiles are preserved across the steeply dipping cores and show several common features: (1) Where long profiles of terraces could be surveyed, the terraces show increased tilts with age. (2) The greatest tilts are preserved toward the core of the folds. (3) The pregrowth strata and the terrace treads are discordant everywhere. (4) The terraces generally are not folded across hinges in the underlying strata.

In combination with previous structural and seismic data, we infer the folds grow by limb rotation within the steeply dipping portion of the folds as new material is translated across the outer hinges of the anticline. We document unambiguous evidence for limb rotation, previously active axial surfaces that are now passive, and younger axial surfaces that remain active as evidenced by fold scarps. In combination with structural data and growth strata, we infer that the width of the Kashi-Atushi folds is established early and that continued shortening is accommodated by vertical growth of the fold via a combination of limb rotation in the center and hinge migration on the flanks. We currently have little age control for the terraces, but if the uplift is roughly equal to the calculated shortening rates across the anticlines, and no regional incision has occurred, the ages of the terraces are 5000–100,000 yr old. Efforts under way to date the terraces will further distinguish spatial patterns of strain rate across folds, the timing of terrace creation with respect to documented climate change, and the kinematic history of fold growth.

ACKNOWLEDGMENTS

Field work was assisted by Shen Jun, Zhao Ruibin, and Dick Heermance. Earlier drafts were improved with insights from Josh Roering and Dick Heermance. We appreciated thorough reviews by

Karl Karlstrom, Lewis Owen, Stuart Hardy, Jerome Van der Woerd, and an anonymous reviewer. This research was supported by the American Association of Petroleum Geologists Grants-In-Aid program, the U.S. National Science Foundation (EAR-9614765, EAR-0230403) and by the National Science Foundation of China (403720081, 49834005).

REFERENCES CITED

Allmendinger, R.W., and Shaw, J.H., 2000, Estimation of fault propagation distance from fold shape: Implications for earthquake hazard assessment: Geology, v. 28, p. 1099–1102, doi: 10.1130/0091-7613(2000)028<1099:EOFPDF>2.3.CO;2.

Atkinson, P.K., and Wallace, K.W., 2003, Competent unit thickness variation in detachment folds in the Northeastern Brooks Range, Alaska: Geometric analysis and a conceptual model: Journal of Structural Geology, v. 25, p. 1751–1771, doi: 10.1016/S0191-8141(03)00003-8.

Biot, M.A., 1964, Theory of internal buckling of a confined multilayered structure: Geological Society of America Bulletin, v. 75, no. 6, p. 563–568.

Bull, W.B., 1991, Geomorphic responses to climatic change: London, Oxford University Press, 326 p.

Casas-Sainz, A.M., Cortes, A.L., and Maestro, A., 2002, Sequential limb rotation and kink-band migration recorded by growth strata, Almazan Basin: North Spain: Sedimentary Geology, v. 146, no. 1–2, p. 25–45, doi: 10.1016/S0037-0738(01)00164-6.

Chen, J., Burbank, D.W., Scharer, K.M., Sobel, E., Jinhui, Y., Rubin, C., and Ruibin, Z., 2002, Magnetochronology of the upper Cenozoic strata in the southwestern Chinese Tian Shan; rates of Pleistocene folding and thrusting: Earth and Planetary Science Letters, v. 195, no. 1–2, p. 113–130, doi: 10.1016/S0012-821X(01)00579-9.

CSB (Chinese Seismological Bureau), 1997, Map of modern seismicity: Chinese Seismological Bureau, scale 1:2,500,000.

Currie, J.B., Patnode, H.W., and Trump, R.P., 1962, Development of folds in sedimentary strata: Geological Society of America Bulletin, v. 73, no. 6, p. 655–673.

Dahlstrom, C.D.A., 1990, Geometric constraints derived from the law of conservation of volume and applied to evolutionary models for detachment folding: American Association of Petroleum Geologists Bulletin, v. 74, no. 3, p. 336–344.

Epard, J.L., and Groshong, R.H., 1995, Kinematic model of detachment folding including limb rotation, fixed hinges and layer-parallel strain: Tectonophysics, v. 247, p. 85–103, doi: 10.1016/0040-1951(94)00266-C.

Ford, M., Williams, E.A., Artoni, A., Verges, J., and Hardy, S., 1997, Progressive evolution of a fault-related fold pair from growth strata geometries, Sant Llorenc de Morunys, SE Pyrenees: Journal of Structural Geology, v. 19, no. 3–4, p. 413–441, doi: 10.1016/S0191-8141(96)00116-2.

Hancock, G.S., and Anderson, R.S., 2002, Numerical modeling of fluvial strath-terrace formation in response to oscillating climate: Geological Society of America Bulletin, v. 114, p. 1131–1142.

Hardy, S., and Finch, E., 2005, Discrete-element modeling of detachment folding: Basin Research, v. 17, p. 507–520, doi: 10.1111/j.1365-2117.2005.00280.x.

Hardy, S., and Poblet, J., 1994, Geometric and numerical model of progressive limb rotation in detachment folds: Geology, v. 22, no. 4, p. 371–374, doi: 10.1130/0091-7613(1994)022<0371:GANMOP>2.3.CO;2.

Holt, W.E., Chamot-Rooke, N., Le Pichon, X., Haines, A.J., Shen-Tu, B., and Ren, J., 2000, Velocity field in Asia inferred from Quaternary fault slip rates and Global Positioning System observations: Journal of Geophysical Research, v. 105, no. B8, p. 19,185–19,209, doi: 10.1029/2000JB900045.

Ishiyama, T., Mueller, K., Togo, M., Okada, A., and Takemura, K., 2004, Geomorphology, kinematic history, and earthquake behavior of the active Kuwana wedge thrust anticline, central Japan: Journal of Geophysical Research, v. 109, p. B12408, doi: 10.1029/2003JB002547.

Jamison, W.R., 1987, Geometric analysis of fold development in overthrust terranes: Journal of Structural Geology, v. 9, p. 207–219, doi: 10.1016/0191-8141(87)90026-5.

Lavé, J., and Avouac, J.P., 2000, Active folding of fluvial terraces across the Siwalik Hills, Himalayas of central Nepal: Journal of Geophysical Research, v. 105, no. B3, p. 5735–5770, doi: 10.1029/1999JB900292.

McClay, K.R., ed., 2004, Thrust tectonics and hydrocarbon systems: Tulsa, Oklahoma, American Association of Petroleum Geologists, 667 p.

Medwedeff, D.A., 1989, Growth of fault-bend folding at Southeast Lost Hills, San Joaquin Valley, California: American Association of Petroleum Geologists Bulletin, v. 73, no. 1, p. 54–67.

Mitchell, M.M., and Woodward, N.B., 1988, Kink detachment fold in the southwest Montana fold and thrust belt: Geology, v. 16, no. 2, p. 162–165, doi: 10.1130/0091-7613(1988)016<0162:KDFITS>2.3.CO;2.

Mitra, S., 2003, A unified kinematic model for the evolution of detachment folds: Journal of Structural Geology, v. 25, no. 10, p. 1659–1673, doi: 10.1016/S0191-8141(02)00198-0.

Molnar, P., Brown, E.T., Burchfiel, B.C., Qidong, D., Xianyue, F., Jun, L., Raisbeck, G.M., Jianbang, S., Zhangming, W., Yiou, F., and Huichuan, Y., 1994, Quaternary climate change and the formation of river terraces across growing anticlines on the north flank of the Tien Shan, China: The Journal of Geology, v. 102, no. 5, p. 583–602.

Nicol, A., and Campbell, J.K., 2001, The impact of episodic fault-related folding on late Holocene degradation terraces along Wairapa River, New Zealand: New Zealand Journal of Geology and Geophysics, v. 44, p. 145–156.

Nicol, A., Van Dissen, R., Vella, P., Alloway, B., and Melhuish, A., 2002, Growth of contractional structures during the last 10 m.y. at the southern end of the emergent Hikurangi forearc basin, New Zealand: New Zealand Journal of Geology and Geophysics, v. 45, p. 365–385.

Novoa, E., Suppe, J., and Shaw, J.H., 2000, Inclined-shear restoration of growth folds: American Association of Petroleum Geologists Bulletin, v. 84, no. 6, p. 787–804.

Pan, B., Burbank, D., Wang, Y., Wu, G., Li, J., and Guan, Q., 2003, A 900 k.y. record of strath terrace formation during glacial-interglacial transitions in northwest China: Geology, v. 31, no. 11, p. 957–960, doi: 10.1130/G19685.1.

Pazzaglia, F.J., and Brandon, M.T., 2001, A fluvial record of long-term steady-state uplift and erosion across the Cascadia forearc high, western Washington State: American Journal of Science, v. 301, no. 4–5, p. 385–431.

Poblet, J., and Hardy, S., 1995, Reverse modeling of detachment folds; applications to the Pico del Aguila anticline in the south central Pyrenees (Spain): Journal of Structural Geology, v. 17, p. 1707–1724, doi: 10.1016/0191-8141(95)00059-M.

Poblet, J., and McClay, K., 1996, Geometry and kinematics of single-layer detachment folds: American Association of Petroleum Geologists Bulletin, v. 80, p. 1085–1109.

Poblet, J., McClay, K., Storti, F., and Munoz, J.A., 1997, Geometries of syntectonic sediments associated with single-layer detachment folds: Journal of Structural Geology, v. 19, no. 3–4, p. 369–381, doi: 10.1016/S0191-8141(96)00113-7.

Poisson, B., and Avouac, J.P., 2004, Holocene hydrological changes inferred from alluvial stream entrenchment in north Tian Shan (northwestern China): The Journal of Geology, v. 112, no. 2, p. 231–249, doi: 10.1086/381659.

Reigber, C., Michel, G.W., Galas, R., Angermann, D., Klotz, J., Chen, J.Y., Papschev, A., Arslanov, R., Tzurkov, V.E., and Ishanov, M.C., 2001, New space geodetic constraints on the distribution of deformation in Central Asia: Earth and Planetary Science Letters, v. 191, p. 157–165, doi: 10.1016/S0012-821X(01)00414-9.

Rockwell, T.K., Keller, E.A., and Dembroff, G.R., 1988, Quaternary rate of folding of the Ventura Avenue anticline, western Transverse Ranges, southern California: Geological Society of America Bulletin, v. 100, p. 850–858, doi: 10.1130/0016-7606(1988)100<0850:QROFOT>2.3.CO;2.

Scharer, K.M., Burbank, D.W., Chen, J., Weldon, R.J., Rubin, C., Zhao, R., and Shen, J., 2004, Detachment folding in the southwestern Tian Shan–Tarim foreland, China: Shortening estimates and rates: Journal of Structural Geology, v. 26, no. 11, p. 2119–2137, doi: 10.1016/j.jsg.2004.02.016.

Schumm, S.A., Mosley, M.P., and Weaver, W.E., 1987, Experimental fluvial geomorphology: New York, John Wiley and Sons, 413 p.

Storti, F., and Poblet, J., 1997, Growth stratal architectures associated to décollement folds and fault-propagation folds; inferences on fold kinematics: Tectonophysics, v. 282, no. 1–4, p. 353–373, doi: 10.1016/S0040-1951(97)00230-8.

Suppe, J., 1983, Geometry and kinematics of fault-bend folding: American Journal of Science, v. 283, p. 684–721.

Suppe, J., and Medwedeff, D.A., 1990, Geometry and kinematics of fault-propagation folding: Eclogae Geologicae Helvetiae, v. 83, p. 409–454.

Suppe, J., Chou, G.T., and Hook, S.C., 1992, Rates of folding and faulting determined from growth strata, *in* McClay, K., ed., Thrust tectonics: London, Chapman and Hall, p. 105–121.

Suppe, J., Sabat, F., Munoz, J.A., Poblet, J., Roca, E., and Verges, J., 1997, Bed-by-bed fold growth by kink-band migration; Sant Llorenc de Morunys, eastern Pyrenees: Journal of Structural Geology, v. 19, no. 3–4, p. 443–461, doi: 10.1016/S0191-8141(96)00103-4.

Thompson, S.C., Weldon, R.J., Rubin, C.M., Abdrakhmatov, K., Molnar, P., and Berger, G.W., 2002, Late Quaternary slip rates across the central Tien Shan, Kyrgyzstan, Central Asia: Journal of Geophysical Research, v. 107, no. 9, p. ETG 7-1–7-32.

Van der Woerd, J., Xiwei, X., Haibang, L., Tapponnier, P., Meyer, B., Ryerson, F.J., Meriaux, A.S., and Zhiqin, X., 2001, Rapid active thrusting along the northwest range front of the Tanghe Nan Shan (western Gansu, China): Journal of Geophysical Research, v. 106, no. B12, p. 30,475–30,504, doi: 10.1029/2001JB000583.

Vannoli, P., Basili, R., and Valensise, G., 2004, New geomorphic evidence for anticlinal growth driven by blind-thrust faulting along the northern Marche coastal belt (central Italy): Journal of Seismology, v. 8, p. 297–312, doi: 10.1023/B:JOSE.0000038456.00574.e3.

Manuscript Received 19 April 2005
Revised Manuscript Received 2 March 2006
Manuscript Accepted 24 March 2006

Printed in the USA